

Chemical, physical and morphological characterization of the electrodeposited iron fragile layer on aluminum substrate

Ivani A. Carlos^{a,*}, Rose M. Carlos, Cecília S. Caruso

^a Departamento de Química, Universidade Federal de São Carlos, CP 676, 13565-905, São Carlos (SP), Brasil

Received 16 July 1996; revised 16 January 1997

Abstract

Compact and fragile iron deposits onto aluminum substrates prepared from a solution of acid chloride were successfully obtained for current densities higher than 0.025 A cm^{-2} and at pH 1.5. Deposits were characterized by cracks which create a good condition to be transformed into a powder. The presence of Cl^- and high acidity that produce deposits with much strain may lead to cracks. The use of aluminum as the cathode must be avoided since its presence is not beneficial to the performance of iron electrodes because of its harmful effect on capacity and charge retention. © 1997 Elsevier Science S.A.

Keywords: Iron deposits; Aluminum substrates

1. Introduction

It is well known that fragile iron electrodeposits can be prepared by electrolysis and this method forms the basis of some industrially sealed preparative routes [1–3]. Fragile iron electrodeposited films have important applications in various technological areas for the manufacturing of permanent magnets [4,5] and for the production of active material of the negative plates of Fe/NiOOH alkaline batteries [6–10]. Electroplating of iron [1–3,11,12] has been carried out in previous studies using four types of plating bath: (i) chlorides; (ii) sulfates; (iii) ammoniacal sulfates, and (iv) by the less-common procedure of the reduction of an iron hydroxide suspension in alkaline media.

Zhelibo et al. [5] produced iron powder using a rotating aluminum disc and an iron chloride solution. Chernov et al. [13] produced iron powder for permanent magnets using iron chloride or iron sulfate solutions and a nickel disc as the cathode.

It should be noted that iron electrodeposits can be contaminated by hydroxides of Fe(II), [1,12,14,15] or by dissolution of metal of the cathode [16–18]. Furthermore, the possibility of corrosion due to the iron deposits being unstable in the electrolytic media or due to the atmospheric oxidation as soon as it has been detached from the cathode, results in another important subject [14–16,18]. Recently, studies of

contamination by electrolytic solution were discussed by Yamashita and Carlos [14,15]. In these studies, iron powder produced from different electrolytic solutions [14,15], indicated that the optimum solution was $\text{FeSO}_4 + \text{CH}_3\text{COONa}$, but the latter produced deposits which became contaminated by iron hydroxides.

In this context, the electrolytic iron deposition studies described here are designed to evaluate the purity of iron powder to be used in the negative plate of Fe/NiOOH alkaline batteries. These studies were carried out taking into account that the presence of some impurities in the battery active material produces the self-discharge of iron electrodes.

2. Experimental

2.1. Substrates

The substrates 1050 Al pieces ($2.0 \text{ cm} \times 2.5 \text{ cm}$), from ALCAN Co. were ground, prior to use, with 600 emery paper and rinsed with distilled water. The '1050 Al alloy' sheet contained 0.25% Si, 0.40% Fe, 0.05% Cu, 0.05% Mn, 0.05% Mg, 0.05% Zn, 0.03% Ti, and traces of other elements: 0.03% X (Ni, Ca, Li, Na, Be, Ti, Pb, B, Zr, Cr, K), and 99.5% Al.

2.2. Film deposition and electrolytic solution

Iron electrodeposits were obtained by cathodic deposition from 1.5 M FeCl_2 at pH 1.5 with HCl. Plating was performed

* Corresponding author.

at room temperature using magnetic stirring controlled at about 1000 rpm. The chronopotentiometric technique was used for the electrodeposition. The range of deposition current density was $0.015\text{--}0.090\text{ A cm}^{-2}$.

2.3. Fragile iron film and iron powder storage

The fragile iron film obtained at 0.090 A cm^{-2} was washed with doubly distilled acetone, dried under nitrogen atmosphere and stored under vacuum using the Schlenk technique. The iron powder was obtained by grinding the iron fragile film in an agate mortar under nitrogen atmosphere and stored by same procedure described above.

2.4. Electrochemical cell

Working electrodes were placed in a conventional three-electrode cell. The counter electrode was a 1010 steel sheet and all potentials were referred to the normal calomel electrode (NCE). The ambient temperature during electrochemical experiments was 25°C . The 1010 steel sheet, from CSN Co., contained 0.04% P, 0.08% C, 0.3% Mn and 0.05% S.

2.5. Instrumentation

Electrochemical measurements were performed under galvanostatic conditions with a PAR Model 173 potentiostat/galvanostat and a ATP/Hi-Teck multimeter. Scanning electron microscopy (SEM) graphs were taken with a Carl Zeiss, Model DSM 940A electron microscopy with 4 nm of resolution connected to an X-ray microanalysis system, Model AN10/55S. X-ray analyses were taken with a diffractometer Model HZ64C and the quantitative analysis was taken in a Interlab spectrophotometer, Model AA12/1475. The surface area of iron powder was determined by the BET method on a CG2000 instrument using nitrogen.

3. Results and discussion

Fig. 1 shows the polarization curves of iron deposition with and without stirring of the deposition bath. The potential shifts to more positive values when the bath is stirred. These results indicate that the deposition process is controlled by mass transport, which is the best condition under which fragile iron deposits are obtained. The low pH of electrolyte solution leads to high evolution of hydrogen which is responsible for the electrochemical efficiency of 78%. Consequently, the pH of electrolyte solution was accurately controlled to avoid Fe(II) hydrolysis. For example, in solutions with pH values higher than 1.5, it was impossible to obtain deposits free of hydroxide contamination leading to current efficiency values higher than 100%. In addition, the anode dissolution allows the concentration of the Fe(II) ions in the electrolyte solution to increase; the pH must be rigorously controlled for this reason. In this context, Fig. 2 shows

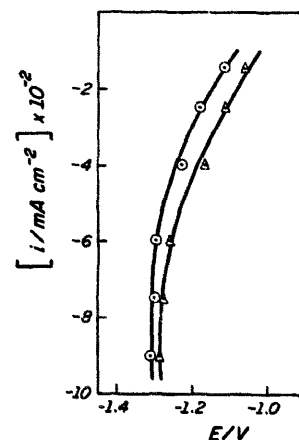


Fig. 1. Steady-state polarization curves for Fe electrodeposition from 1.5 M $\text{FeCl}_2 \cdot 4\text{H}_2\text{O}$ at pH 1.5 with HCl solutions (O) without and (Δ) with magnetic stirring (1000 rpm).

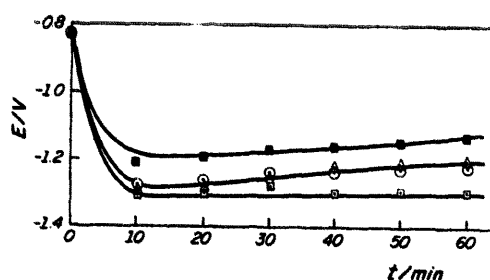


Fig. 2. Galvanostatic profiles of iron electrodeposition process obtained at same $i_d = 0.090\text{ A cm}^{-2}$: (□) 1st, (Δ) 7th, (O) 8th, (■) 9th electrodepositions. Electrolytic solution 1.5 M $\text{FeCl}_2 \cdot 4\text{H}_2\text{O}$ at pH 1.5.

the influence of the increase in Fe(II) concentration versus the galvanostatic curves of iron electrodeposition by dissolution of the anode at a current density of 0.090 A cm^{-2} . These results show that the increase in Fe(II) concentration in solution make the deposition potential shift to more positive values.

Figs. 3–5 show the physical characterization of the electrodeposited iron film at 0.090 A cm^{-2} by SEM. Fig. 3 shows that the iron deposits are not homogeneous since they present compact and spongy regions. Fig. 4 shows that the compact

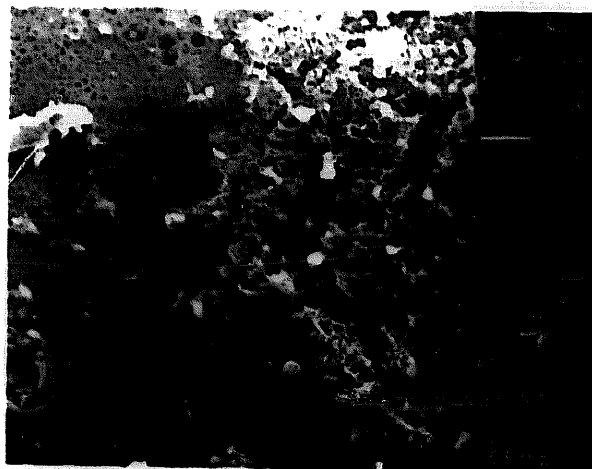


Fig. 3. SEM graphs of iron deposit; electrolytic solution 1.5 M $\text{FeCl}_2 \cdot 4\text{H}_2\text{O}$ at pH = 1.5, $i_d = 0.090\text{ A cm}^{-2}$.



Fig. 4. SEM graphs of iron deposit in region of the cracks; electrolytic solution 1.5 M FeCl₂ · 4H₂O at pH = 1.5, *i*_d = 0.090 A cm⁻².

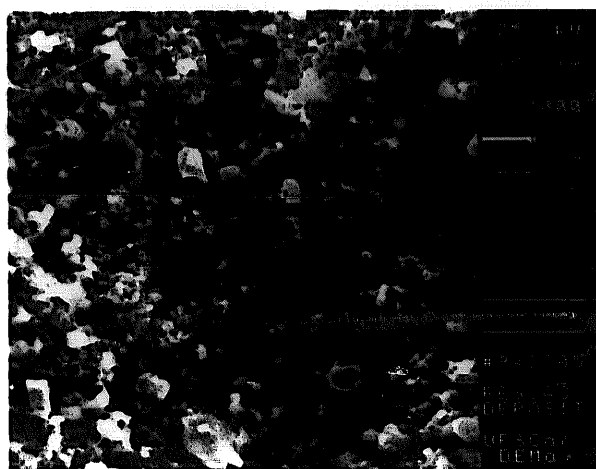


Fig. 5. SEM graphs of spongy iron deposit; electrolytic solution 1.5 M FeCl₂ · 4H₂O at pH = 1.5, *i*_d = 0.090 A cm⁻².

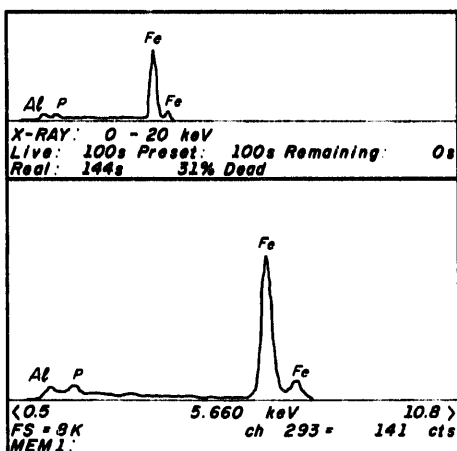


Fig. 6. EDX analysis of iron deposit in the region without incrustation; electrolytic solution 1.5 M FeCl₂ · 4H₂O at pH = 1.5, *i*_d = 0.090 A cm⁻².

region of the iron deposit presents many cracks and white incrustations. These cracks, in principle, weaken the deposit but they are fundamental to transform the deposit into powder form. It seems that the existence of these cracks has been offered by the presence of Cl⁻ and the high acidity of the

electrolyte solution which produce deposits with many strain leading to cracks [1]. As shown in Fig. 5 the spongy regions present also white incrustations. These white incrustations (Figs. 3–5) probably come from the aluminum alloy cathode.

Energy dispersion X-ray (EDX) analyses were taken in order to obtain a better characterization of the iron deposits. As shown in Fig. 6 the iron deposit regions without white incrustation present aluminum and phosphorus impurities. Fig. 7 shows that iron deposit regions containing white incrustations have aluminum, phosphorus and also potassium impurities. These contaminants can be produced by the cathode dissolution in HCl medium and by the oxidation of the anode in the electrochemical cell. The white incrustation is probably Al(OH)₃ obtained by the reaction of Al³⁺ ion and OH⁻ ion since the evolution of hydrogen in the metal/electrolyte interface increases the pH of the solution.

The presence of phosphorous species in the iron deposits are not harmful to the Fe/NiOOH batteries but the presence of aluminum species have a detrimental effect, especially on the iron electrode when it is present in an amount greater than 0.01% [19]. Atomic absorption spectrophotometry (AAS) showed that the iron contamination represents 0.1% of the total aluminum. The harmful effect on capacity and charge retention of the iron electrodes is due to the reaction of Al³⁺ with the OH⁻ of the electrolyte solution producing

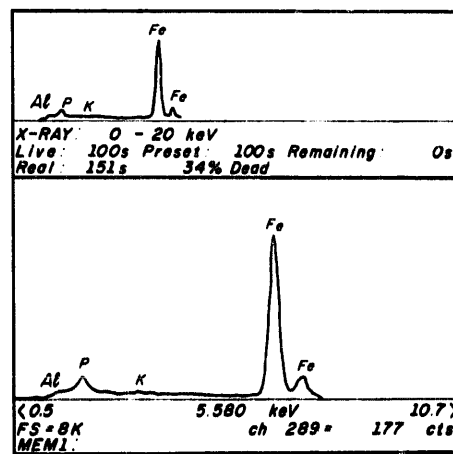


Fig. 7. EDX analysis of iron deposit in the region containing incrustations; electrolytic solution 1.5 M FeCl₂ · 4H₂O at pH = 1.5, *i*_d = 0.090 A cm⁻².

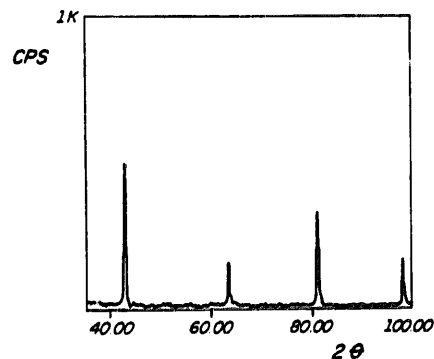


Fig. 8. X-ray analysis of powder iron; electrolytic solution 1.5 M FeCl₂ · 4H₂O at pH = 1.5, *i*_d = 0.090 A cm⁻².

Table 1
Experimental interplanar distances (d_{exp}) of the x-ray diffraction peaks of iron powder and the corresponding theoretical interplanar distances (d_t) [20]

| d_{exp} | $(I/I_0)_{\text{exp}}$ (%) | Fe | | Fe/Al | | Al | |
|------------------|-------------------------------|-------|--------------------|-------|--------------------|-------|--------------------|
| | | d_t | $(I/I_0)_t$ (%) | d_t | $(I/I_0)_t$ (%) | d_t | $(I/I_0)_t$ (%) |
| 2.060 | 100 | 2.030 | 100 | 2.040 | 100 | 2.024 | 55 |
| 1.117 | 66 | 1.170 | 30 | 1.180 | 90 | 1.196 | 1 |
| 1.446 | 29 | 1.430 | 20 | 1.450 | 80 | 1.450 | 1 |
| 1.018 | 28 | 1.030 | 10 | 1.180 | 90 | | |

[Al(OH)₄]⁻. The probable source of potassium species in the iron deposits is the aluminum alloy cathode, but it seems that its presence does not create problems.

Fig. 8 shows X-ray diffraction patterns of iron powder. In Table 1 the main experimental and theoretical results of the interplanar distances, d , [20] of α -Fe and the Fe–Al alloy are compiled for comparison. These results show that the peak at $d=2.06$ ($I/I_0=100\%$) can be attributed either to α -Fe or the Fe–Al alloy. The peaks at $d=1.446$ ($I/I_0=29\%$) and $d=1.018$ ($I/I_0=28\%$) are attributed to α -Fe since their intensities are not only lower than those found for Fe–Al alloy $d=1.45$ ($I/I_0=80\%$) and $d=1.08$ ($I/I_0=90\%$) but also lower than half of the Fe–Al alloy peaks intensities. The peak at $d=1.17$ ($I/I_0=66\%$) is attributed to the Fe–Al alloy, $d=1.02$ ($I/I_0=70\%$). These results show that iron electro-deposits consist of α -Fe and Fe–Al alloy. This alloy is obtained during the electrodeposition of iron on the aluminum alloy substrate.

BET results show that iron deposits which were transformed into powder have an area of $4 \text{ m}^2 \text{ g}^{-1}$. They have a low value when compared with the area of commercial ARMICO iron powder, $9 \text{ m}^2 \text{ g}^{-1}$ [9]. As the superficial area is an important parameter for the Fe/NiOOH battery plates, this can be optimized by using other forms of grinding such as a ball mill, because iron deposits obtained using high acidity (pH: 1.5) are difficult to grind with agate mortar.

4. Conclusions

Compact and fragile iron deposits onto aluminum substrates prepared from an acid chloride solution were success-

fully obtained for current densities higher than 0.025 A cm^{-2} and at pH 1.5. It was shown that the atmospheric oxidation of the fragile iron film can be controlled by washing it with doubly distilled acetone, drying under nitrogen atmosphere and storing under vacuum using the Schlenk technique. Physical and chemical characterization of the iron fragile deposits have shown that electrolytic iron was contaminated by aluminum alloy substrate. Since the amount of aluminum obtained is greater than the allowed value for Fe/NiOOH batteries this aluminum alloy substrates should be avoided.

References

- [1] R. Colasaru, *Electrodeposition of Metal Powders*, Elsevier, Amsterdam, 1979.
- [2] F.A. Lowenheim, *Modern Electroplating*, Wiley, New York, 2nd edn., 1974.
- [3] N.V. Parthasaday, *Practical Electroplating Handbook*, Prentice-Hall, Englewood Cliffs, NJ, 1989.
- [4] R. Walker and A.R.B. Sandford, *Chem. Ind.*, 6 (1979) 642.
- [5] E.P. Zhelibo, T.V. Chubar, T.N. Amelichkina, E.L. Khandros and V.V. Myalkovhina, *Sov. Powder Metale Met. Ceram.*, 13 (1973) 777.
- [6] K. Vijayamohan, A.K. Shukla and K. Sathyanarayana, *J. Power Sources*, 32 (1990) 329.
- [7] P. Kabanov, *Discuss. Faraday Soc.*, 1259 (1947) 263.
- [8] J. Cerný, J. Jindra and K. Micha, *J. Power Sources*, 45 (1993) 267.
- [9] C.A.C. Souza, *Ph.D. Thesis*, Universidade Federal de São Carlos, Brasil, 1994.
- [10] A.J. Salking, C.J. Venuto and S.V. Falk, *J. Electrochem. Soc.*, 11 (1964) 493.
- [11] C.M. Chu and C.C. Wan, *J. Mater. Sci.*, 27 (1992) 6700.
- [12] L. Dommikov, *Met. Finishing*, (1971) 40.
- [13] G.K. Chernov, A.I. Polishchuck, V.K. Shikin, R.V. Balandina, T.G. Sheremetseva and V.M. Konykhova, *Sov. Powder Metal Ceram.*, 12 (1973) 179.
- [14] E.M. Yamashita and I.A. Carlos, *1a Jornada Regional Iniciação Científica, Brasil, 1991*, p. 47.
- [15] E.M. Yamashita and I.A. Carlos, *15a Reunião Anual Sociedade Brasileira de Química, Brasil, 1992*.
- [16] C.S. Caruso, C.A. Caldas and I.A. Carlos, *16a Reunião Anual Sociedade Brasileira de Química, Brasil, 1993*.
- [17] C.S. Caruso and I.A. Carlos, *2a Cong. Iniciação Científica, UFSCAR, Brasil, 1994*.
- [18] C.S. Caruso and I.A. Carlos, *18a Reunião Anual Sociedade Brasileira de Química, Brasil, 1995*.
- [19] S.V. Falk and A.J. Saling, *Alkaline Storage Batteries*, Wiley, New York, 1969, p. 629.
- [20] *Joint Committee on Powder Diffraction Standards, JCPDS*.